

Scientific Article

Modeling of chronic radiation-induced cystitis in mice

Bernadette M.M. Zwaans PhD^a, Sarah Krueger PhD^{a,b},
Sarah N. Bartolone MS^a, Michael B. Chancellor MD^{a,b,c},
Brian Marples PhD^{a,b}, Laura E. Lamb PhD^{a,b,*}

^a Beaumont Health System, Royal Oak, Michigan

^b Oakland University William Beaumont School of Medicine, Auburn Hills, Michigan

^c Lipella Pharmaceuticals, Pittsburgh, Pennsylvania

Received 13 June 2016; received in revised form 18 July 2016; accepted 25 July 2016

Abstract

Purpose: Radiation cystitis (RC), a severe inflammatory bladder condition, develops as a side effect of pelvic radiation therapy in cancer patients. There are currently no effective therapies to treat RC, in part from the lack of preclinical model systems. In this study, we developed a mouse model for RC and used a Small Animal Radiation Research Platform to simulate the targeted delivery of radiation as used with human patients.

Methods and materials: To induce RC, C3H mice received a single radiation dose of 20 Gy delivered through 2 beams. Mice were subjected to weekly micturition measurements to assess changes in urinary frequency. At the end of the study, bladder tissues were processed for histology.

Results: Radiation was well-tolerated; no change in weight was observed in the weeks after treatment, and there was no hair loss at the irradiation sites. Starting at 17 weeks after treatment, micturition frequency was significantly higher in irradiated mice versus control animals. Pathological changes include fibrosis, inflammation, urothelial thinning, and necrosis. At a site of severe insult, we observed telangiectasia, absence of uroplakin-3 and E-cadherin relocalization.

Conclusions: We developed an RC model that mimics the human pathology and functional changes. Furthermore, radiation exposure attenuates the urothelial integrity long-term, allowing for potential continuous irritability of the bladder wall from exposure to urine. Future studies will focus on the underlying molecular changes associated with this condition and investigate novel treatment strategies.

Copyright © 2016 the Authors. Published by Elsevier Inc. on behalf of the American Society for Radiation Oncology. This is an open access article under the CC BY-NC-ND license (<http://creativecommons.org/licenses/by-nc-nd/4.0/>).

Sources of support: This work was supported by the Urology Care Foundation Research Scholars Program for B.M.M.Z. and funded in part by grant (R44DK102247) from the National Institute of Diabetes and Digestive and Kidney Diseases through a subcontract from Lipella Pharmaceuticals.

Conflicts of interest: B.M.M.Z. is a Urology Care Foundation Scholar. M.B.C. is the founder and chief scientific officer of Lipella Pharmaceuticals, Inc. The remaining authors declare that they have no other relevant financial interests.

Study received approval from the Beaumont Health System Research Institute institutional animal care committee.

* Corresponding author. Beaumont Research Institute, 3811 W. 13 Mile Road, Suite 187, Royal Oak, MI 48073

E-mail address: Laura.lamb@beaumont.edu (L.E. Lamb)

<http://dx.doi.org/10.1016/j.adro.2016.07.004>

2452-1094/Copyright © 2016 the Authors. Published by Elsevier Inc. on behalf of the American Society for Radiation Oncology. This is an open access article under the CC BY-NC-ND license (<http://creativecommons.org/licenses/by-nc-nd/4.0/>).

Introduction

Radiation is often used to manage pelvic malignancies, either as primary or (neo)adjuvant treatment. Management options include external beam radiation therapy or brachytherapy, with the former more appropriate to patients with intermediate- or high-risk disease.^{1,2} External beam radiation therapy aims to deliver the highest possible dose of radiation to cancer cells while sparing normal surrounding tissues and organs. Despite substantial advances in image guidance that allow better radiation dose distributions and improve treatment accuracy, external beam radiation therapy may still result in some degree of normal tissue damage. Irradiation-induced bladder injury can lead to the development of radiation cystitis (RC), a chronic bladder inflammation characterized by hematuria. RC is a debilitating condition that can severely degrade a cancer survivor's quality of life and require long-term follow-up and treatment. Symptoms associated with this condition include urinary frequency, urgency, nocturia, pain, incontinence, reduced bladder capacity, and hematuria. The degree of hematuria can range from microscopic to life-threatening.^{3,4} In 2016, approximately 34% of newly diagnosed cancers are expected to arise in the pelvis.⁵ Of the patients with pelvic tumors receiving radiation treatment, 15% to 20% will develop bladder complications within 10 years after treatment.^{6,7} Risk factors for developing radiation toxicity include radiation dose, fraction, and field size, as well as age at exposure, genetic variations, concurrent therapies, and comorbidities such as diabetes and immunodeficiency.⁸ There are currently no effective therapies to treat radiation-induced hemorrhagic cystitis, and, although rare, it is a severe condition with substantial morbidity and risk of mortality.

RC is a severe inflammatory condition of the bladder that consists of three phases. An initial acute inflammatory response generally lasts only a few weeks after radiation therapy. This phase is followed by a symptom-free phase that can last from months to years. The third, irreversible, chronic phase represents a range of clinical symptoms for which there is no standard management.^{4,9} Histologically, this phase is characterized by an influx of inflammatory cells, endarteritis, thinning of the urothelial wall, edema, collagen deposition, loss of smooth muscle cells, and some degree of hemorrhaging.⁴ Current treatment options include rest/hydration, clot evacuation, continuous irrigation, hyperbaric oxygen therapy, blood transfusion, botulinum toxin injections, and, as a last resort, formalin instillation or cystectomy.^{3,4,9} The effectiveness of these therapies is limited and the recurrence rate is high; furthermore, these treatments are mainly focused on arresting hemorrhaging and do not target other lower urinary tract symptoms (eg, urgency, frequency, nocturia).

The limited success of current treatment options is due in part to the absence of preclinical models that mimic the

human condition and the lack of understanding the molecular changes that are responsible for the disease progression. Several animal models for RC have been described⁴; however, there is variety in radiation delivery systems, difference in the delivered dose, and dose distribution, along with species used in these disparate studies. Furthermore, most studies lack functional analysis of the bladder in response to irradiation. In this study, we used the Small Animal Radiation Research Platform (SARRP) to closely recapitulate the targeted external beam radiation therapy that human cancer patients receive.⁴ Through a single dose of 20 Gy, divided over 2 beams delivered directly to the bladder, we were able to induce long-term damage to the bladder that coincided with increased urinary frequency and decreased bladder capacity as seen in patients with RC.

Methods and materials

Animals

All experimental procedures were reviewed and approved by the Institute Animal Care and Use Committee. Eight-week-old C3H/HeN mice (Charles River) were housed under standard housing conditions with 5 mice per cage, fed a soy protein-free extruded rodent diet, and cages that were changed weekly. The C3H/HeN mouse strain was chosen because it is considered to be fibrosis-prone in response to radiation.¹⁰ Female mice were used for these studies because male mice are known to mark their territory with urine, thereby interfering with the micturition studies.

Radiation treatment

Radiation was performed on the SARRP unit (Xstrahl Life Sciences) using image-based targeting of the bladder. Twenty mice received a single radiation dose of 20 Gy and 20 mice served as controls. The 20 Gy dose was chosen based on previous studies by others using the same mice strain and reliability of detecting radiation-induced DNA damage (gamma-H2AX) in the bladder model.¹¹⁻¹⁴ The selection of this dose was also driven by pragmatic reasons of model development and also to allow data comparison with previous studies.^{11-13,15-18} Finally, and most relevant, is that the standard of care (SOC) for external beam radiation therapy for intermediate- or high-risk prostate cancer is 2 Gy of daily fractions to a total dose of 70 to 74 Gy.¹⁹ Using an α/β value of 2 Gy for prostate cancer, the calculated biologically effective dose (BED) is 148 Gy (for SOC of 2 Gy in 37 fractions to 74 Gy). This is a comparable BED for a single dose of 20 Gy in the bladder using an $\alpha/\beta = 3$ Gy (BED = 153 Gy for late-responding normal tissues).²⁰

For SARRP imaging and irradiation, mice were anesthetized using isoflurane to maintain precise positioning. Immediately before treatment, a computed tomography (CT) scan was taken and the target for irradiation set in the middle of the bladder. Bladder treatments were performed without the use of contrast to avoid incorrect dosimetry calculations, which are based on CT values. For treatments, confirmation of targeting and beam position was made visually by experienced operators who had familiarity with proper animal positioning (to avoid normal structures) as well as knowledge of the location and physical characteristics of the mouse bladder on CT (Fig 1A). A 5 × 5 mm collimator was used to provide full bladder coverage and the isocenter was set consistently in the center of the bladder, which is easily visualized on orthogonal CT views. Typical beams were opposed laterals at 140°. They were angled by the operator to try to avoid the spine, long bones in the legs, and normal gut/rectum as much as possible; beams were minorly adjusted as needed for each animal (Fig 1B).

Treatment planning software (Muriplan, similar to that used in radiation therapy of human patients) was used to determine the precise beam arrangement to focus the total dose on the bladder alone. Imaging and irradiation for each animal was accomplished within 30 to 60 minutes. Following successful irradiation, mice recovered in a warming tank and were returned to general housing.

To validate treatment targeting, CT imaging and treatment planning was performed with and without CT contrast in a few test subjects. Multiple possible treatment plans (2 or 3 beams, arc, 5 × 5 or 10 × 10 collimator) were compared using dose-volume histograms in the treatment planning software. The 2-beam treatment provided the best ratio of bladder coverage to normal tissue damage and so was chosen for the larger study of 40 mice outlined above.

Micturition assay

Once per week, mice were placed into metabolic cages for overnight voiding measurements from 4 PM until 8 AM (16 hours). These times were chosen because rodents are nocturnal and the mouse bladder reaches peak capacity between 7 PM and 1 AM.²¹ Metabolic cages allow free access to food and water and provide a means for separating urine from feces. Urine was collected on a pH-sensitive paper affixed to the underside of the cage to distinguish between urine and water drops. After 16 hours, the animal was returned to general housing and the paper was removed for analysis. pH-sensitive paper was scanned in color, urinary frequency was calculated by quantifying the number of urine spots on the paper, and urine output was estimated by measuring the surface area of the urine spots and comparing it with a standard curve of known volume/area measurements using a Photoshop

counting tool. The moving average of 3 consecutive weekly measurements was calculated and plotted. Significance was calculated using a multiple *t* test.

Immunohistochemistry

Animals were sacrificed when irradiation-induced increased micturition changes were observed. Upon sacrifice, bladders were instilled with 100 µL of 4% formaldehyde, dissected, and fixed for 24 hours at 4°C. Subsequently, bladders were cut in half longitudinally and processed for histology at the University of Michigan Unit of Laboratory Animal Medicine in vivo animal core facility.

The 4-µm sections were subjected to hematoxylin and eosin (H&E), Masson Trichrome (fibrosis; TRM-2, SCY TEK Laboratories), or toluidine blue (mast cells; T3260, Sigma) staining. Additionally, slides were immunostained for uroplakin-3 (ab78196, Abcam), platelet/endothelial cell adhesion molecule-1 (PECAM-1)/CD31 (ab124432, Abcam), and E-cadherin (ab76055, Abcam). All slides were warmed to 61°C to melt paraffin and subjected to a series of deparaffinization and rehydration steps. Trichrome and toluidine blue stains were performed according to the manufacturer's instructions. For the immunostaining, antigen retrieval was performed in sodium citrate buffer pH 6.0 and peroxidase activity was blocked in 3% hydrogen peroxide in methanol for 15 minutes. For uroplakin-3 and E-cadherin detection, the M.O.M. kit (PK-2200, Vector Labs) was used according to the manufacturer's instructions, with a 15-minute incubation for primary antibodies. For CD31, slides were incubated in blocking buffer (1% bovine serum albumin, 0.1% cold fish skin gelatin, 0.5% triton X-100, 0.05% sodium azide in phosphate-buffered solution) for 1 hour, exposed to primary antibody diluted in blocking buffer for 15 to 30 minutes, and washed in phosphate-buffered solution containing 0.05% Tween20. Antibody signal was enhanced using the ABC detection system (Vector Labs, PK-4001), visualized with Immimpact DAB (Vector Labs, SK-4105), and counterstained with hematoxylin.

Data analysis

H&E sections were scored by a blinded veterinary pathologist (Unit of Laboratory Animal Medicine in-vivo animal core facility, University of Michigan) for the presence of fibrosis, urothelial thinning, ischemic necrosis and inflammation. The lesions were graded based on severity: minimal, mild, moderate, and severe (score 1 through 4, respectively). Inflammation was defined by the presence of polymorphonuclear cells, lymphocytes, plasma cells, and/or macrophages, and sections were scored based on the number of inflammatory cells present: absent, minimal (rare, 1 to 5 cells), mild (at least 10 fields with 6 to 20 cells), moderate (at least 10 fields with 20 to 50 cells), or marked (packed with cells).

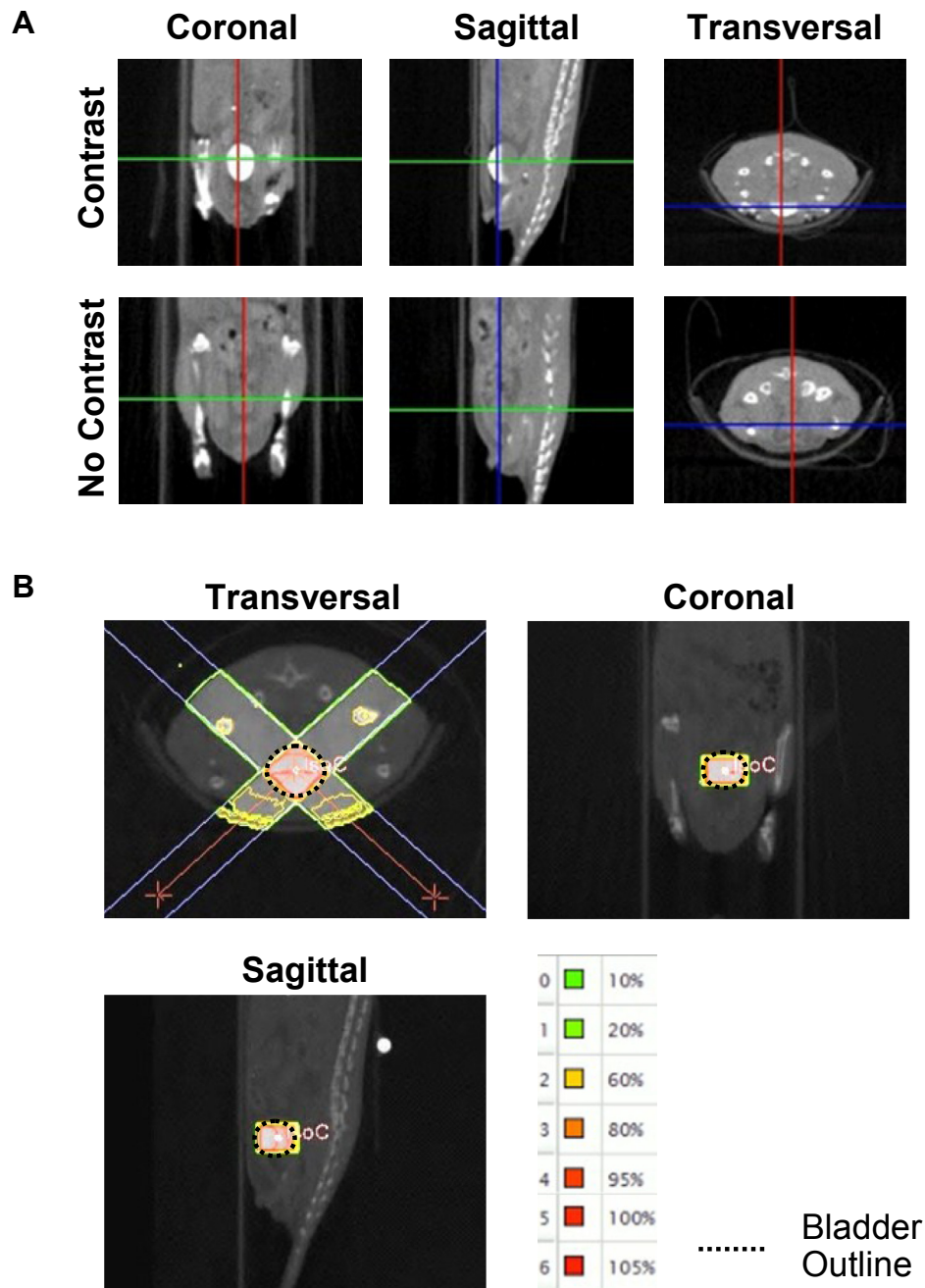


Figure 1 Small animal radiation research platform setup. (A) Bladder computed tomography imaging in the presence and absence of instilled contrast fluid. (B) Small Animal Radiation Research Platform treatment computed tomography with typical treatment beam arrangement and isodose distribution for 20 Gy. A ventral beam entry was chosen to reduce dose to the long bones of the legs. Two beams of 5×5 mm were used to spread dose to skin on entry and exit points. The bladder has been outlined with a black dotted line for ease of visualization.

For trichrome and uroplakin-3 staining, 6 representative images were taken per slide and scored by 2 blinded scientists. The degree of fibrosis identified with Masson trichrome stain was classified as normal/mild or moderate/severe. Uroplakin-3 staining was classified as present or absent. All data points were processed in GraphPad and statistical significance was calculated using the multiple *t* test.

Results

Targeted radiation induces an increase in micturition frequency

Female C3H mice received a single dose of 20 Gy irradiation targeting directly to the bladder using SARRP.

Mice tolerated radiation well; no change in overall health or body weight was observed in the weeks after irradiation (Fig 2A). Approximately 20% of mice suffered from some degree of alopecia, ranging from minor alopecia on their back to almost full body hair loss. Alopecia was observed in both irradiated and nonirradiated animals, and, in irradiated mice, areas of hair loss did not correlate with areas of radiation exposure. In addition, alopecia is a common phenotype of the C3H mouse strain and thus we conclude that the hair loss was unrelated to irradiation exposure.²² One irradiated mouse died at 11 weeks after irradiation; the cause was undefined at necropsy.

Weekly micturition measurements were performed using pH-sensitive paper and metabolic cages, with the first placement in the metabolic cages at 1 week before irradiation treatment. This measurement was used as a baseline measurement; the last micturition measurement was performed at 19 weeks after irradiation (Fig 2B). A significant increase in micturition resulting from radiation exposure was observed starting at 17 weeks after irradiation (Fig 2C-D). To correct for variation in water consumption, we calculated the average urine volume per micturition event. The increased micturition frequency coincided with a decrease in urine volume per micturition event in the irradiated mice (Fig 2E), indicating that the elevated frequency is independent of the amount of water consumed and may possibly be due to reduced bladder capacity.

Radiation-induced pathological damage to the bladder

Bladder tissues from 6 mice per treatment group were randomly selected for pathological analysis. H&E staining was scored (score, 0-4) blinded by a pathologist for fibrosis, inflammation, urothelial thinning, and ischemic necrosis.^{4,9} No change in bladder size was noted in response to irradiation. Bladder irradiation resulted in a long-term mild increase in each of these pathological changes (Fig 3). Normal bladder tissue consists of the urothelium and the detrusor muscle, separated by the lamina propria, which is in part made up of connective tissue, vasculature, lymphatic vessels, nerve endings, and surveilling immune cells (eg, macrophages). Irradiation causes long-term damage to all 3 layers of the bladder wall. The most prominent long-term pathological change observed upon exposure is the buildup of fibrous tissue in the lamina propria and between muscle cells (Fig 4). Additionally, a mild increase in inflammatory cells was detected in response to irradiation (Fig 4). Other observed pathological changes include edema, loss of endothelial cells, urothelial hyperplasia, and hemorrhaging (Fig 4).

Masson trichrome stain revealed a modest increase in fibrosis in irradiated bladders in comparison to control

tissue (Fig 5; not significant). Mast cells play a role in the early phase of radiation-induced inflammation and promote fibrosis.²³ However, toluidine blue staining did not reveal a significant influx of mast cells in response to irradiation in our model (Fig 6).

The mouse urothelium, typically made up of 2 to 3 layers of urothelial cells and a single layer of umbrella cells, was reduced to a single cell layer or even completely lost in the majority of irradiated bladder tissues (urothelial thinning; Fig 3). To visualize the urothelium, bladder sections were stained with the urothelial differentiation marker uroplakin-3, which is expressed in the superficial umbrella cells and some intermediate urothelial cells. Uroplakin-3 staining was lost in 60% of irradiated bladder samples (Fig 7A). However, the absence of uroplakin-3 was not indicative of urothelial thinning as lack of uroplakin-3 was also observed in hyperplastic regions (Fig 7A).

Long-term loss of urothelial integrity in response to radiation

Hematuria is a prominent symptom of RC, ranging from microscopic to gross hematuria. In chronic RC, hematuria is characterized by telangiectatic blood vessels and endarteritis that result in fibrosis and leaky blood vessels.^{7,9,12} Underneath the urothelium is a dense capillary plexus that, in addition to providing the urothelium with blood supply, protects the detrusor from substances that penetrate through the urothelium. To test for vascular changes in response to radiation, bladder tissues were stained for PECAM-1/CD31. Overall, no striking differences were found in blood vessel density and size in response to irradiation (data not shown). However, telangiectasia, small dilated blood vessels, was apparent in an area of severe damage (Fig 7B). A urine dipstick test revealed no sign of hematuria (data not shown). To assess if increased bladder permeability in this region could drive this vascular response, we determined the expression of uroplakin-3 and the cell-adhesion molecule E-cadherin in this region. Both factors contribute to the impermeable properties of the urothelium.²⁴⁻²⁶ Uroplakin-3 expression was significantly reduced in this hyperplastic region and E-cadherin localization shifted from being strictly membrane bound to high a cytoplasmic abundance without altering expression levels (Fig 7B). These changes indicate that attenuation of urothelial integrity is a long-term side effect from radiation treatment and could contribute to vascular changes seen in RC.

Discussion

Medical advances in early cancer diagnosis and treatment are leading to improved cancer survival rates. The number of cancer survivors in the United States is

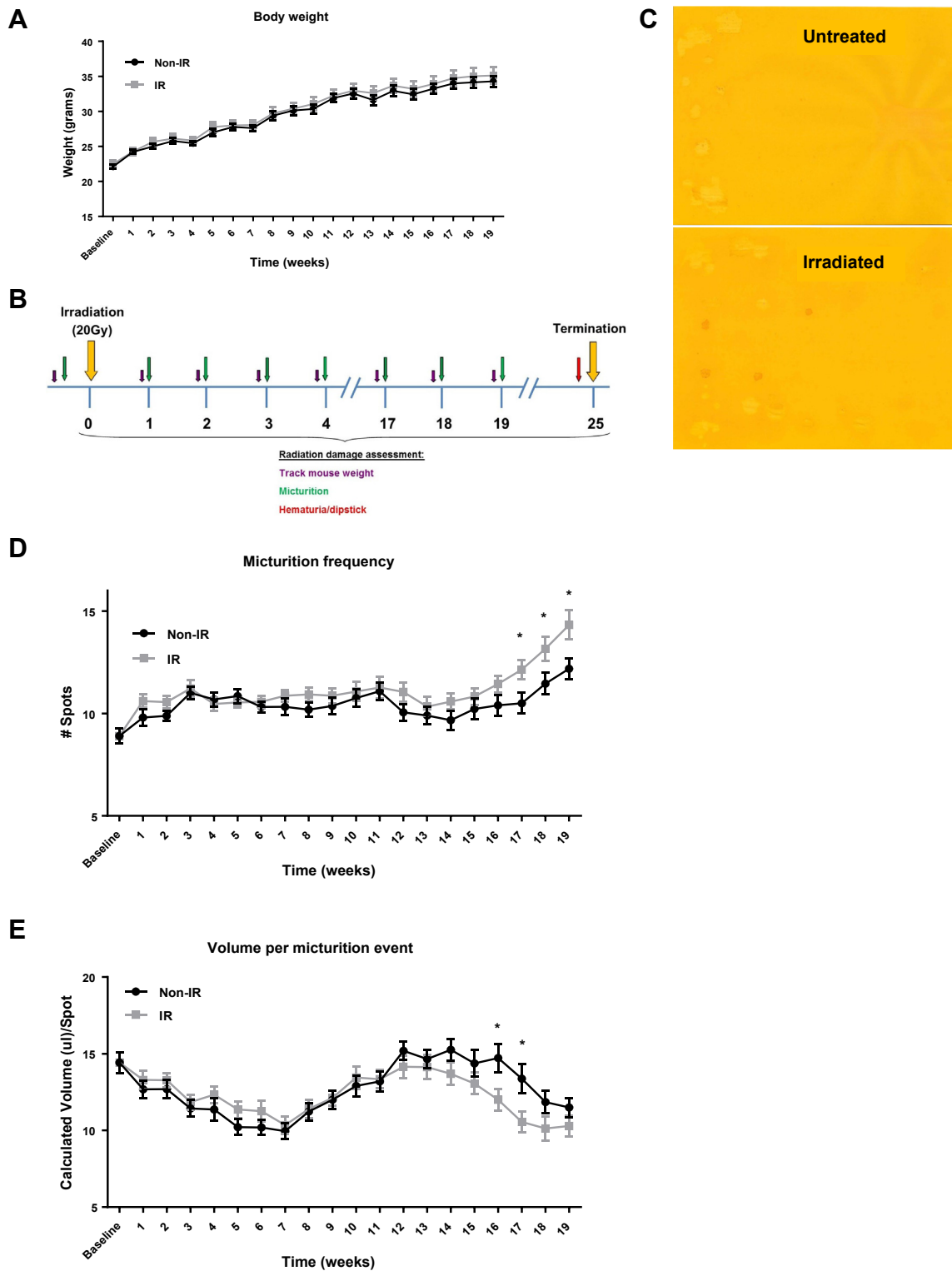


Figure 2 Delayed increase in micturition frequency after radiation exposure. (A) Average weekly mouse weights throughout the experimental phase were graphed. (B) Timeline of the conducted animal study. (C) Representative images of pH-sensitive paper at the end of a micturition study at 17 weeks after irradiation (IR) exposure. (D) The moving average of weekly measurements of micturition frequency and (E) volume per micturition event over 19 weeks were calculated and plotted. $n = 20$ per treatment group; $*P < .05$ (multiple t test); error bars = standard error of the mean.

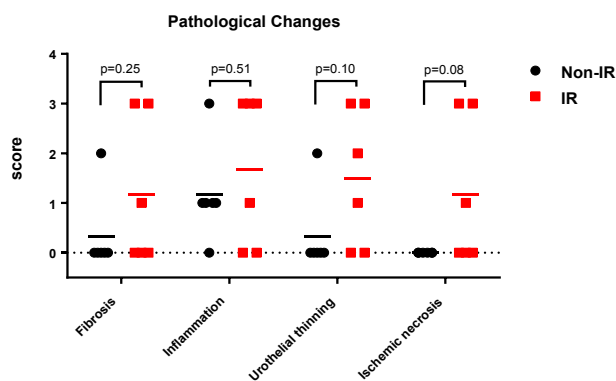


Figure 3 Irradiation (IR)-induced chronic pathologic damage to the bladder. Bladder tissues were scored by a pathologist for fibrosis, inflammation, urothelial thinning, and ischemic necrosis on a scale from 0 to 4 (0 = absent, 4 = severe; n = 6 per treatment group).

expected to rise to almost 30% between 2016 and 2026.²⁷ As a result, the side effects of cancer treatments such as chemoradiation and radiation therapies are becoming more apparent and are creating a new challenge for health care providers. One such side effect is radiation cystitis, a severe debilitating chronic inflammatory bladder condition caused by exposure to pelvic irradiation.

Our goal was to develop a mouse model of RC that recapitulates the functional and pathological changes seen in humans by using SARRP. SARRP uses CT imaging and a multiple external radiation beam approach to accurately deliver radiation while limiting radiation exposure to normal tissues. This technique was previously applied successfully by our research team in a rat model for acute RC, in which radiation lowered intermicturition intervals in a dose-dependent manner.²⁸ In

the current study, we show that a single treatment of 20 Gy in C3H/HeN mice causes a significant increase in micturition frequency starting at 17 weeks after irradiation while simultaneously reducing the volume per micturition event. These findings suggest that the increased frequency is due to reduced bladder capacity. Acute inflammation, cell death, and necrosis in early RC causes irreversible fibrosis, thereby reducing bladder elasticity; subsequently, the patient presents with lower urinary tract symptoms such as urgency, frequency, and nocturia.^{4,7} The increased radiation-induced micturition in our mouse model was supported by a mild increase in fibrosis (Fig 3 and 4). The lack in significant difference in fibrosis between the 2 treatment groups was possibly from the low number of animals included in the study. In addition, a modest increase in inflammation was noted (no statistical significance). The lack of a strong inflammatory and fibrotic response could be dose-dependent because radiation-induced damage is positively correlated with the total dose^{16,28}; thus, a higher dose or extension of the study will likely result in a more severe phenotype. Furthermore, the influx of inflammatory cells, such as mast cells, and edema are characteristics of acute RC and thus might not be apparent long-term after irradiation.⁴

Damage to the vasculature plays a pronounced role in the development of hematuria and is the leading cause of extensive complications in patients with RC. Endothelial cells have a slow turnover rate; thus, radiation-induced vascular damage only becomes apparent in late RC. Changes in the vasculature include loss of endothelial cells, endarteritis, fibrosis around blood vessels, telangiectasia, and hemorrhaging, of which we observed endothelial cell loss, hemorrhaging, and telangiectasia in our severe cases (Fig 4). Restoring the bladder

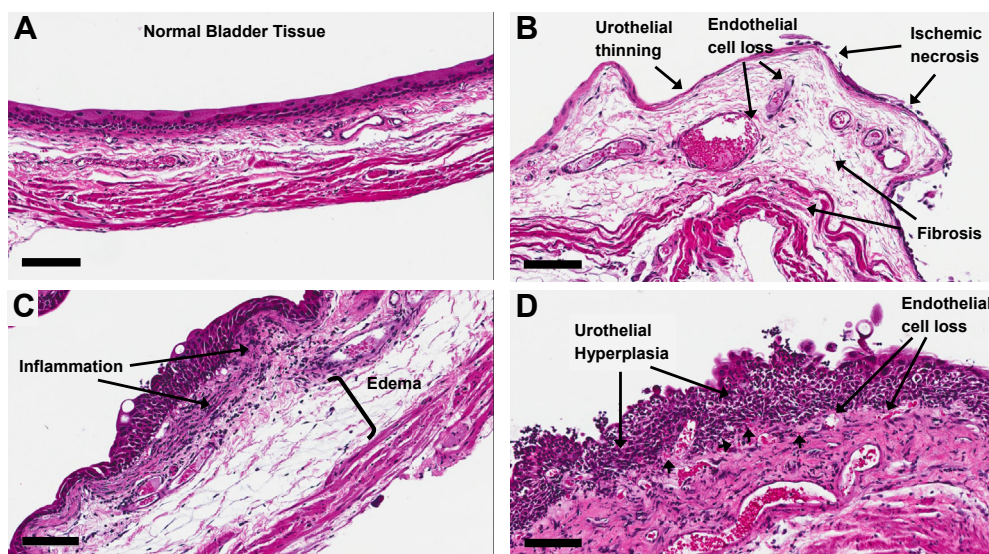
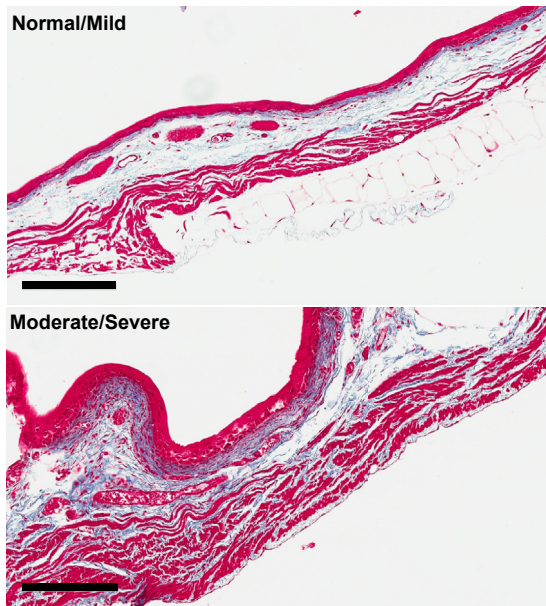


Figure 4 Hematoxylin and eosin staining of normal (A) and irradiated bladder (B-D) tissues are shown with indicated pathological changes. Arrowheads point at sites of hemorrhaging. Black bar, 100 μm.



	Non-IR	IR	P-Value
Normal/ Mild	87.5% n=7/8	57.1% n=4/7	0.211
Moderate/ Severe	12.5% n=1/8	42.9% n=3/7	

Figure 5 Accumulation of fibrous tissue in response to radiation treatment. Untreated and irradiated (IR) bladder samples were stained with Masson trichrome stain, thereby giving fibrous tissue a blue color. Bladder tissues were scored for the degree of fibrosis by 2 scientists blinded to the process and classified as normal/mild or moderate/severe fibrosis. n = 8 and n = 7 for non-IR and IR groups, respectively.

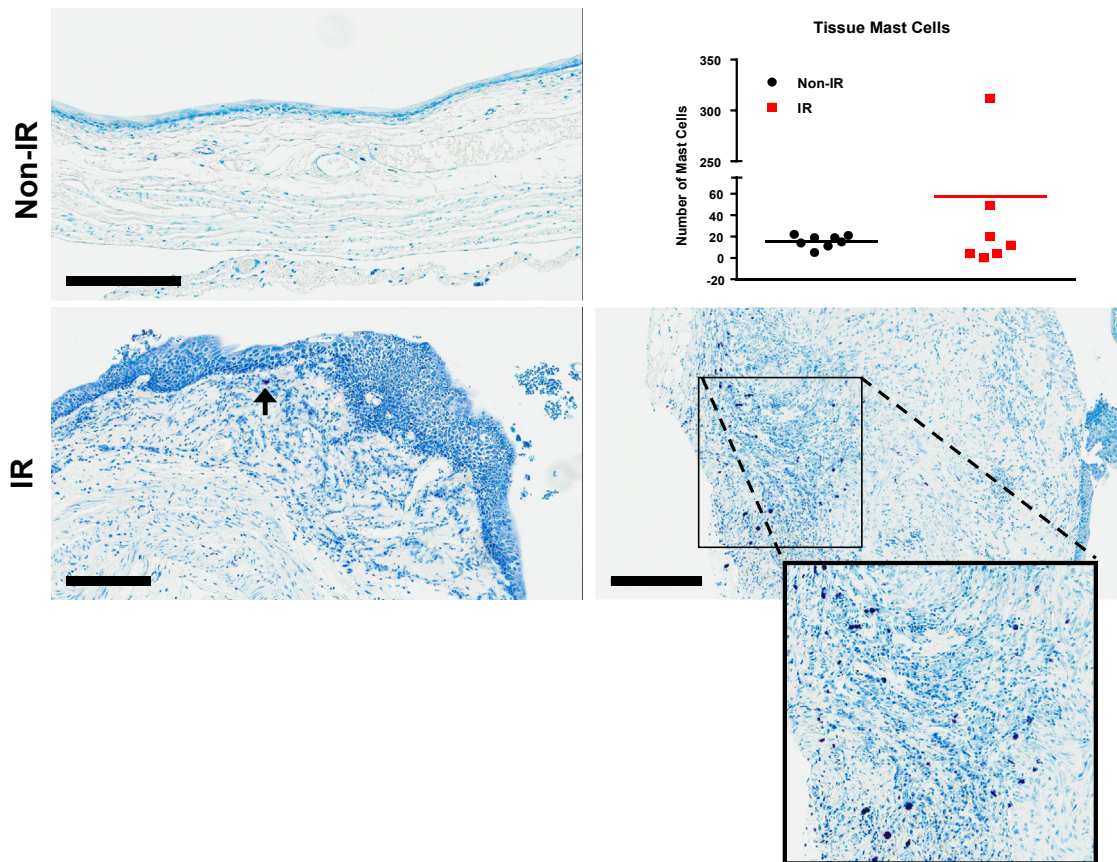


Figure 6 Influx of mast cells in areas of severe radiation-induced urothelial damage. Normal and irradiated bladder tissues were stained with Toluidine blue (nuclei = blue; mast cells = purple). Total number of mast cells was counted in two full bladder cross sections per sample. Arrow indicates purple stained mast cell. N=8 and n=7 for non-IR and IR groups respectively; black bar = 200µm.

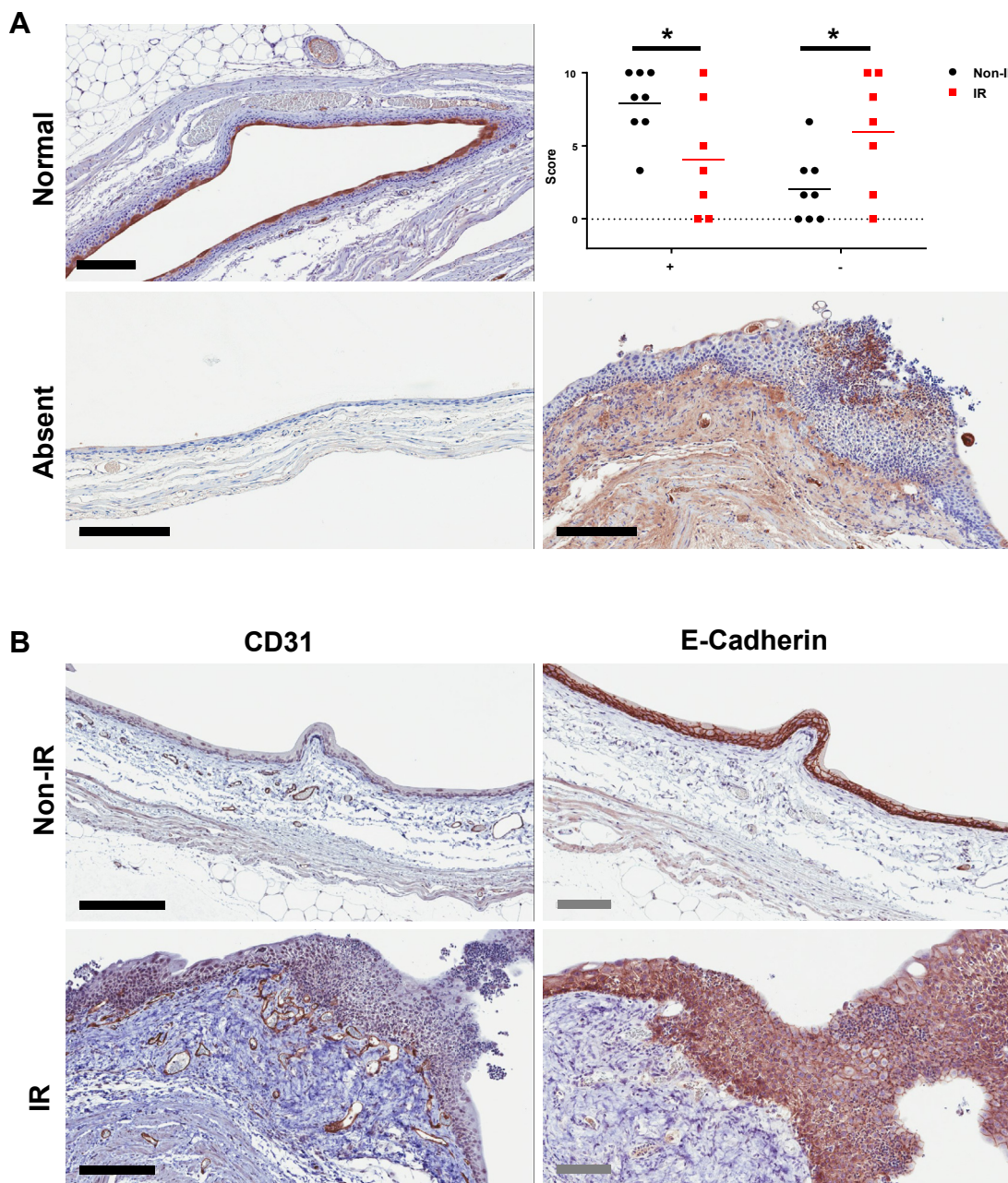


Figure 7 Irradiation (IR)-induced bladder damage correlates with hypervascularization and loss of bladder integrity. (A) Normal and IR bladder tissue were stained for uroplakin-3. Six images per tissue sample were scored (1-10) blinded by 2 independent scientists for the presence or absence of uroplakin-3. n = 8 and n = 7 for non-IR and IR treatment groups, respectively. (B) Normal tissues and areas of severe radiation-induced damage to the urothelium were stained for blood vessels (CD31) and E-cadherin. Gray bar, 100 μm, black bar, 200 μm; **P* < .05 (multiple *t* test).

vasculature in patients with RC is an active area of research. Novel approaches include neovascularization techniques such as hyperbaric oxygen therapy and injection of vascular endothelial growth factor and/or endothelial cells, as well as blood coagulation therapies including estrogen, GreenLight XPS laser therapy, and intravesical liposomal formulation of tacrolimus and prostaglandin instillations.⁴

Furthermore, we found that irradiation causes long-term damage to the urothelium, which is visible through thinning of the urothelial layer and focal areas of ischemic necrosis (Fig 4). The bladder has the unique ability to store large quantities of urine while maintaining a high level of impermeability. Numerous factors in the urothelium contribute to bladder impermeability, including uroplakin proteins and tight junctions.^{25,26,29} When these

factors are compromised, a severe inflammatory condition of the bladder can arise.³⁰ Therefore, we sought to determine if radiation can affect the integrity of the bladder urothelium long-term. In addition to a loss of urothelial cells, our study found reduced uroplakin-3 expression in irradiated urothelium (Fig 7A). Likewise, at sites of severe damage, E-cadherin, a major component of tight junctions, was redistributed from the cellular membrane to the cytoplasm without compromising E-cadherin expression levels (Fig 7B). Cellular redistribution of E-cadherin may be an indication that radiation disrupts tight junction formation long-term. Further studies are needed to understand the consequences of these urothelial changes and to investigate the efficacy of targeted therapy to protect the urothelium (eg, hyaluronic acid) for RC patients.^{31,32}

Another C3H substrain (C3H/Neu) was previously used to model RC.¹¹⁻¹³ Similar to our current study, mice were exposed to a single dose of 20 Gy, causing increased collagen deposition, urothelial thinning, and progressive loss of uroplakin-3 expression. However, in this model, a single vertical beam using an Isovolt 320/20 X-ray machine was used to target the bladder. This technique has a number of limitations when compared with our study. First, it has a higher degree of localized collateral damage in surrounding tissues of the single planar beam than would be expected in the current 2-planar beam study. Second, the 20-Gy bladder dose in the current study was calculated using image-guided treatment planning software that was not available at the time of the previous studies, giving a higher degree of dosimetry confidence. This mouse model is a useful tool to further characterize radiation-induced changes in the bladder and to test novel treatment modalities.

Despite the evidence of RC-related symptoms in our SARRP-irradiated mouse bladders, a number of limitations to the study should be noted. First, the method used to quantify micturition frequency does not account for timing of the urination events or for the possible movement of the mouse during urination. Second, as described earlier, RC has a triphasic development: an early acute phase, followed by an indolent symptom-free phase, and a chronic irreversible phase. In our study, we did not observe significant changes in micturition immediately after radiation treatment. Although it is unclear if the patients with chronic RC always have a history of acute RC, it is feasible that a higher radiation dose will reveal an acute response. In addition, a higher dose will likely also intensify the functional and histological changes observed in this study. Finally, we acknowledge that the method used to calculate micturition volume is not strictly quantitative. However, other described methods are either invasive (eg, placement of an indwelling catheter) or do not allow for natural bladder behavior (eg, taking a mouse out of its own environment).^{33,34}

Conclusion

In this study, we developed a chronic RC model that simulates the human condition. This is the first mouse study that uses SARRP for bladder irradiation to closely mimic human patients. Radiation exposure resulted in increased micturition frequency and histological changes including fibrosis, urothelial damage, inflammation, and necrosis. Furthermore, we demonstrated that radiation exposure attenuates the urothelial integrity long-term, allowing for continuous irritability of the bladder wall from exposure to urine. Future studies will focus on the underlying molecular changes associated with this condition and investigate novel treatment strategies to help patients with radiation cystitis.

Acknowledgments

We thank Andrew Vereecke, Peter Levanovich, Dr. Heinz Nicholas, and the Radiation Cystitis Foundation for their thoughtful discussions on our radiation cystitis modeling and translational research efforts. This study received approval from the Beaumont Health System Research Institute institutional animal care committee.

References

1. D'Amico AV, Whittington R, Malkowicz SB, et al. Biochemical outcome after radical prostatectomy, external beam radiation therapy, or interstitial radiation therapy for clinically localized prostate cancer. *JAMA*. 1998;280:969-974.
2. Shipley WU, Thames HD, Sandler HM, et al. Radiation therapy for clinically localized prostate cancer: A multi-institutional pooled analysis. *JAMA*. 1999;281:1598-1604.
3. Payne H, Adamson A, Bahl A, et al. Chemical- and radiation-induced haemorrhagic cystitis: Current treatments and challenges. *BJU Int*. 2013;112:885-897.
4. Zwaans BM, Chancellor MB, Lamb LE. Modeling and treatment of radiation Cystitis. *Urology*. 2016;88:14-21.
5. American Cancer Society. *Cancer Facts and Figures 2016* Volume 2016. Atlanta: American Cancer Society; 2016.
6. American Cancer Society. *Cancer Treatment & Survivorship Facts & Figures 2014-2015*. Atlanta: American Cancer Society; 2014.
7. Manikandan R, Kumar S, Dorairajan LN. Hemorrhagic cystitis: A challenge to the urologist. *Indian J Urol*. 2010;26:159-166.
8. Shadad AK, Sullivan FJ, Martin JD, Egan LJ. Gastrointestinal radiation injury: Symptoms, risk factors and mechanisms. *World J Gastroenterol*. 2013;19:185-198.
9. Smit SG, Heyns CF. Management of radiation cystitis. *Nat Rev Urol*. 2010;7:206-214.
10. Chen ES, Greenlee BM, Wills-Karp M, Moller DR. Attenuation of lung inflammation and fibrosis in interferon-gamma-deficient mice after intratracheal bleomycin. *Am J Respir Cell Mol Biol*. 2001;24:545-555.
11. Jaal J, Dorr W. Radiation induced inflammatory changes in the mouse bladder: The role of cyclooxygenase-2. *J Urol*. 2006;175:1529-1533.
12. Jaal J, Dorr W. Radiation induced late damage to the barrier function of small blood vessels in mouse bladder. *J Urol*. 2006;176:2696-2700.

13. Jaal J, Dorr W. Radiation-induced damage to mouse urothelial barrier. *Radiother Oncol*. 2006;80:250-256.
14. Wong J, Armour E, Kazanzides P, et al. High-resolution, small animal radiation research platform with x-ray tomographic guidance capabilities. *Int J Radiat Oncol Biol Phys*. 2008;71:1591-1599.
15. Dorr W, Schultz-Hector S. Early changes in mouse urinary bladder function following fractionated X irradiation. *Radiat Res*. 1992;131:35-42.
16. Kraft M, Oussoren Y, Stewart FA, Dorr W, Schultz-Hector S. Radiation-induced changes in transforming growth factor beta and collagen expression in the murine bladder wall and its correlation with bladder function. *Radiat Res*. 1996;146:619-627.
17. Kanai AJ, Zeidel ML, Lavelle JP, et al. Manganese superoxide dismutase gene therapy protects against irradiation-induced cystitis. *Am J Physiol Renal Physiol*. 2002;283:F1304-F1312.
18. Soler R, Vianello A, Fullhase C, et al. Vascular therapy for radiation cystitis. *Neurourol Urodyn*. 2011;30:428-434.
19. Dearnaley D, Syndikus I, Mossop H, et al. Conventional versus hypofractionated high-dose intensity-modulated radiotherapy for prostate cancer: 5-year outcomes of the randomised, non-inferiority, phase 3 CHHiP trial. *Lancet Oncol*. 2016;17(8):1047-1060.
20. Thames HD, Bentzen SM, Turesson I, Overgaard M, Van den Bogaert W. Time-dose factors in radiotherapy: A review of the human data. *Radiother Oncol*. 1990;19:219-235.
21. Dorr W. Cystometry in mice—influence of bladder filling rate and circadian variations in bladder compliance. *J Urol*. 1992;148:183-187.
22. Schurch B, de Seze M, Denys P, et al. Botulinum toxin type a is a safe and effective treatment for neurogenic urinary incontinence: Results of a single treatment, randomized, placebo controlled 6-month study. *J Urol*. 2005;174:196-200.
23. Zheng H, Wang J, Hauer-Jensen M. Role of mast cells in early and delayed radiation injury in rat intestine. *Radiat Res*. 2000;153:533-539.
24. Choi SH, Byun Y, Lee G. Expressions of uroplakins in the mouse urinary bladder with cyclophosphamide-induced cystitis. *J Korean Med Sci*. 2009;24:684-689.
25. Hu P, Meyers S, Liang FX, et al. Role of membrane proteins in permeability barrier function: Uroplakin ablation elevates urothelial permeability. *Am J Physiol Renal Physiol*. 2002;283:F1200-F1207.
26. Zhang CO, Wang JY, Koch KR, Keay S. Regulation of tight junction proteins and bladder epithelial paracellular permeability by an antiproliferative factor from patients with interstitial cystitis. *J Urol*. 2005;174:2382-2387.
27. Miller KD, Siegel RL, Lin CC, et al. Cancer treatment and survivorship statistics, 2016. *CA Cancer J Clin*. 2016;66:271-289.
28. Rajaganapathy BR, Janicki JJ, Levanovich P, et al. Intravesical liposomal tacrolimus protects against radiation cystitis induced by 3-beam targeted bladder radiation. *J Urol*. 2015;194:578-584.
29. Hu P, Deng FM, Liang FX, et al. Ablation of uroplakin III gene results in small urothelial plaques, urothelial leakage, and vesicoureteral reflux. *J Cell Biol*. 2000;151:961-972.
30. Slobodov G, Feloney M, Gran C, Kyker KD, Hurst RE, Culkin DJ. Abnormal expression of molecular markers for bladder impermeability and differentiation in the urothelium of patients with interstitial cystitis. *J Urol*. 2004;171:1554-1558.
31. Shao Y, Lu GL, Shen ZJ. Comparison of intravesical hyaluronic acid instillation and hyperbaric oxygen in the treatment of radiation-induced hemorrhagic cystitis. *BJU Int*. 2012;109:691-694.
32. Gacci M, Saleh O, Giannesi C, et al. Bladder instillation therapy with hyaluronic acid and chondroitin sulfate improves symptoms of postradiation cystitis: Prospective pilot study. *Clin Genitourin Cancer*. In press.
33. Kurien BT, Everds NE, Scofield RH. Experimental animal urine collection: A review. *Lab Anim*. 2004;38:333-361.
34. Sessions A, Eichel L, Kassahun M, Messing EM, Schwarz E, Wood RW. Continuous bladder infusion methods for studying voiding function in the ambulatory mouse. *Urology*. 2002;60:707-713.